Size effect of He clusters on the interactions with self-interstitial tungsten atoms at different temperatures*

Jinlong Wang(王金龙)[1,†], Wenqiang Dang(党文强)[2,‡], Daping Liu(刘大平)[1], and Zhichao Guo(郭志超)[1]

[1]*Department of Physics, Xinxiang University, Xinxiang* 453003, *China*
[2]*Department of Physics, Tianshui Normal University, Tianshui* 741000, *China*

(Received 31 March 2020; revised manuscript received 21 May 2020; accepted manuscript online 25 May 2020)

The behaviors of helium clusters and self-interstitial tungsten atoms at different temperatures are investigated with the molecular dynamics method. The self-interstitial tungsten atoms prefer to form crowdions which can tightly bind the helium cluster at low temperature. The crowdion can change its position around the helium cluster by rotating and slipping at medium temperatures, which leads to formation of combined crowdions or dislocation loop locating at one side of a helium cluster. The combined crowdions or dislocation loop even separates from the helium cluster at high temperature. It is found that a big helium cluster is more stable and its interaction with crowdions or dislocation loop is stronger.

Keywords: helium cluster, self-interstitial, tungsten, molecular dynamics simulation

PACS: 31.15.xv, 61.80.Jh, 61.82.Bg **DOI:** 10.1088/1674-1056/ab9619

1. Introduction

Tungsten (W) has been used as a plasma-facing material (PFM) in International Thermal Nuclear Fusion Experimental Reactor (ITER) due to its high melting point, high thermal conductivity and low sputtering erosion.[1,2] Tungsten as a PFM can be irradiated by high-energy (14.1 MeV) neutrons, hydrogen (H) and helium (He) ions. The energy of mixed H–He plasma is up to 100 eV, and the fluxes on the order of 10^{24} He $m^{-2}\cdot s^{-1}$.[3] The transient surface temperature of tungsten can be up to 3000 K.[4] Irradiation of helium on tungsten surface is now considered to be an important problem in fusion reactors.[5] Bombardment of helium ions can result in the retention and formation of helium clusters, dislocation loops and fuzz on tungsten surface,[4,6–9] which degrade the mechanical properties (embrittlement and hardness)[10,11] and thermal conductivity of tungsten, and finally drastically reduce the service life of PFM.[12] Thus, to assess long-term performance of a PFM, it is necessary to understand the behavior of helium in tungsten. In recent years, the behavior of helium in tungsten has been studied extensively in experiments and simulations. About the behaviors of helium in tungsten, the migration energy of He is very low, around 0.06 eV, and the He–He binding energy is found to be ∼1.09 eV at a distance of ∼1.5 Å.[13] The binding energies of He in tungsten are always positive,[14–16] which leads to growth of helium clusters by self-trapping[17] and coalescence between helium clusters.[18,19] The small interstitial helium clusters are mobile, which can be attracted to tungsten surfaces and grain boundary due to an elastic interaction force that drives segregation.[20,21] The migration energies of He_n ($1 \leq n \leq 6$) clusters calculated by empirical potential are 0.15 eV to 0.45 eV.[22] "Trap mutation" is a process in which interstitial helium clusters create Frenkel defect pairs and occupy vacancies.[23–25] Helium clusters become immobile when they are trapped by vacancy or trap mutation occurs.[26,27] First-principles calculations suggested that a single W vacancy can contain at least nine He atoms.[28] High temperature can promote growth of helium clusters and occurrence of trap mutations (the He/V ratio decreases with increasing temperature).[17,29] Pentecoste *et al.*[30] found that the diffusion, formation and coalescence of clusters lead to the flak of the substrate, which explains the saturation of the retention observed experimentally.

About the behaviors of tungsten self-interstital atoms (SIAs), Mason *et al.* found that the nanometer scale dislocation loops are predominantly of prismatic $1/2\langle 111\rangle$ type during the early stage of self-ion irradiation with *in situ* transmission electron microscopy (TEM).[31] The calculation results of density functional theory (DFT) reveal that the smaller solute transition metal atoms favorably bond to the $\langle 111\rangle$ crowdion.[32] The molecular dynamics (MD) simulation showed that the migration of SIA is very fast, and the migration energy is calculated to be 0.013 eV.[33] The SIAs can rotate and rearrange to form dislocation loop around a helium cluster.[23,24] The rotation energy barriers of SIA_n for $1 \leq n \leq 7$ are 0.67–2.7 eV in pristine tungsten.[34]

On the interactions between SIAs and helium clusters, growth of a helium cluster is accompanied by the formation

*Project supported by the Young Scientists Fund of the National Natural Science Foundation of China (Grant No. 11705157), the Henan Provincial Key Research Projects, China (Grant No. 17A140027), and the Ninth Group of Key Disciplines in Henan Province of China (Grant No. 2018119).

†Corresponding author. E-mail: 396292346@qq.com
‡Corresponding author. E-mail: 530262320@qq.com

of SIAs and dislocation loop.[27,35] The dislocation loop generally bind with the helium cluster while occasionally diffuse away under certain conditions.[23] Hammond *et al.* showed that dislocation loop attracts and traps helium in the tensile region (parallel to the Burgers vector) but repels helium in the compressive regions (along the direction of Burges vector).[36] Li *et al.* found that the presence of SIA can promote helium clusters to capture more additional He atoms.[37] The DFT calculation showed that the binding energy between helium and an SIA is as high as 0.94 eV.[14] Sandoval *et al.* showed that the growth rate of helium clusters will affect the distribution of SIAs.[38] Slow growth rates allow the diffusion of interstitials around the bubble, while the interstitials do not have time to diffuse with fast growth rates, leading to a more isotropic growth.

The dislocation loop slides and annihilates on the surface forming structures of adatom 'islands', which is conceived to be active in the initial stages of fuzz growth.[23] Kajita *et al.*[39] showed that the fuzz structure forms on the tungsten surface over the temperature range from 900 K to 2000 K. Only micrometer-sized holes form on the tungsten surface at the temperature above 2000 K.[40] Using object kinetic Monte Carlo (OKMC) simulation, Valles *et al.*[41] showed that the great majority of helium atoms are retained in monovacancies at low temperatures, which prevents the growth of helium clusters. At higher temperatures, helium atoms and vacancies are emitted from small He_nV_m clusters ($n < 40$, $m < 10$), also preventing the formation of larger helium clusters and the growth of fuzz. These investigations reveal that the temperature has significant effects on the growth of helium clusters and formation of fuzz.

It is helpful to understand the growth of He clusters by studying the behavior of He clusters and their surrounding SIAs. However, until now, the research in this aspect is very limited, such as the stability of helium cluster and the behaviors of SIAs at different temperatures. Modeling and simulation are important complementary tools to study the atomic behavior of helium in metals. The atomic simulation method can provide the information about energy, interaction, microstructure, mechanism and so on. In this work, we investigate the behaviors of helium cluster and self-interstitial tungsten atom at different temperatures using the molecular dynamics method.

2. Methodology

All the simulations are performed using the parallel molecular dynamic (MD) package LAMMPS.[42] Visualization of atomic configuration is used with the open vizualization tool OVITO.[43] The tool "Wigner-Seitz defect analysis" embedded in the OVITO[43] is used to determine the number of Frenkel defects. The inter-atomic potential used in the present work is the same as described in Ref. [44]. The potential of Juslin *et al.*[45] and Bonny *et al.*[44] accurately reproduces the *ab initio* results of the formation energies and ground states of helium and crowdion. However, the potential of Juslin and Wirth[45] provides a helium migration barrier of 0.21 eV, which overestimates the DFT value (0.06 eV) by more than three times. Thus we finally decide to use the potential of Bonny *et al.* The simulation box is $20a \times 20a \times 20a$, which contains 16000 tungsten atoms, where a is the lattice constant of tungsten to be 3.14 Å. Periodic boundary conditions are used in all simulations.

In order to explore the different configurations that He_n clusters can adopt. We use a method similar with that of adapting by Boisse *et al.*[17] Boisse obtained the possible configurations of helium clusters by molecular dynamics evolution at 1000 K. For every 100 steps, the simulation box is minimized thus obtaining a large set of minimum configurations. The configuration adopted by helium clusters with the lowest potential energy are determined finally. We obtain the possible configurations using parallel replica dynamics (PRD)[46,47] method in the temperature range 300–1500 K. The PRD is one of accelerated dynamics methods that is suitable for infrequent-event systems. All the possible configurations generated from the PRD calculation are performed in energy minimization, from which the configuration with the lowest potential energy is determined. We obtain the most stable configuration by repeatedly running PRD. It should be noted that normally we randomly add an extra helium atom based on the previous stable configuration to find the next configuration. For example, we add an extra helium based on the He_{12}'s configuration to find the most stable configuration of the He_{13} cluster. Sometimes, we randomly put n helium atoms in a small region at the center of the simulation box as the initial configuration to run PRD to check out the results. It is found that the most stable configurations of He_4, He_6, He_{13}, He_{26} and He_{55} clusters in tungsten have high symmetry. As shown in Fig. 1, the configuration of the He_4 cluster is a regular tetrahedron, the He_6 cluster is a regular octahedron, the He_{13} cluster is a regular icosahedron, and the He_{55} cluster is a bigger regular icosahedron, in which the He_{13} cluster inside it. The He_{26} cluster also has high symmetry and its size falls between He_{13} and He_{55} clusters. According to the atomic colors in Fig. 1, the big helium cluster should be more stable, which is further justified in the following discussion. Thus we select these helium clusters as representatives to study the behaviors of helium clusters and self-interstitial atoms with the temperature range 300–3500 K.

It has been proved that the isolated dissolved helium atoms prefer to accumulate by self-trapping.[13,24] Thus the He_n cluster is directly introduced in the center of the simulation box within a sphere region with radius of 0.2 Å in order

to save time for calculating the agglomeration process. Then we perform an energy minimization and equilibrium with an isothermal-isobaric ensemble of *NPT* (density, pressure, temperature). Finally, the system evolves for a long time. The Frenkel defect, crowdion and dislocation loop form during the process of energy minimization, temperature equilibrium and evolution. We output an atomic structure once in a while during the evolution to inspect the atomic structures. It should be noted that the crowdions and dislocation loop formed in the vicinity of the helium cluster are very difficult to identify, especially at high temperature due to the severe atomic thermal vibration. Hence we perform energy minimization for each snapshot in order to inspect the atomic configurations clearly. In addition, it should be noted that the final atomic configuration after the current temperature evolution serves as the initial configuration to evolve with higher temperature. For example, the final atomic configuration of He_6 after evolving ~467 ps at 300 K serves as the initial configuration to evolve at 1000 K.

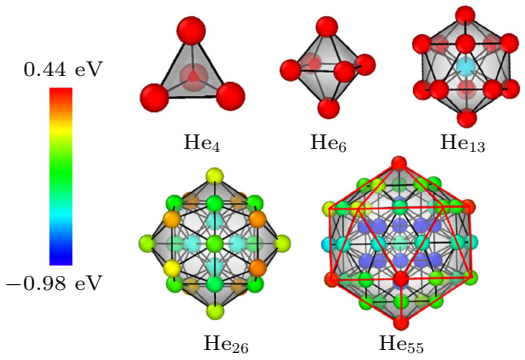

Fig. 1. The most stable configuration of He_4, He_6, He_{13}, He_{26} and He_{55} clusters in tungsten. The balls represent helium atoms and the black sticks connect two helium atoms within the distance of 2.0 Å. The rainbow colors of the balls represent the atomic potential energies from −0.98 eV (blue) to 0.44 eV (red). The surface mesh is constructed and the transparency is 50% in order to show clearly.

3. Results and discussion

The average binding energy $E_{\text{ave-b}}$ and trapping energy E_{trap} are defined as follows:

$$E_{\text{ave-b}} = \frac{1}{n}(E_{\text{W+He}_n} + (n-1)E_{\text{W}} - nE_{\text{W+He}}), \quad (n \geq 2) \quad (1)$$

$$E_{\text{trap}} = E_{\text{W+He}_n} + E_{\text{W}} - E_{\text{W+He}_{n-1}} - E_{\text{W+He}}, \quad (n \geq 2) \quad (2)$$

where $E_{\text{W+He}_n}$, $E_{\text{W+He}}$, and E_{W} represent the system's total energy of the He_n cluster in tungsten, one He in tungsten and tungsten. According to our definition, the negative values represent the binding energy. The average binding energy and trapping energy represent the ability for helium atoms to bind together and for the helium cluster to trap an extra helium atom. The average binding energy and trapping energy versus the size of the helium cluster are shown in Fig. 2. The average binding energies decrease gradually with the size, revealing the increase of stability of the helium cluster. The average binding energies seem to converge to a certain value according to the current trend. The trapping energies show the trend similar to the average binding energy, while they also show strong capture capability at certain sizes (at 4, 6, 13, 18, 19, and so on). The calculations of Boisse *et al.* using DFT and empirical potential also show strong trapping energy and similar trend for He_n clusters ($2 \leq n \leq 16$).[17] The trapping energies are generally stronger using the current interatomic potential.

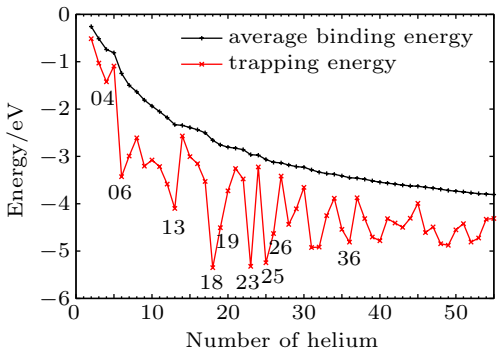

Fig. 2. The average binding energy and trapping energy versus the size of the helium cluster.

The prefactor $\hat{\nu}$ is calculated to be 2.86×10^{-6} $m^2 \cdot s^{-1}$ for the He_4 cluster according to the conventional Arrhenius [$D = \hat{\nu}\exp(-\Delta E/k_B T)$] behavior.[22] In this work, the He_4 cluster migrates about 6.95 Å at 300 K during ~596 ps, and even dissociates into several isolated helium atoms at 1500 K. The high mobility of the He_4 cluster is due to no trap mutation occurring, and it remains to be an interstitial cluster. This is consistent with the DFT results,[17] in which the He_n clusters occur trap mutation for n larger than 6. Another study also showed that, when $n \geq 6$, the high pressure caused by the He_n cluster is conceived sufficiently to kick out a tungsten atom from the lattice position, forming the immobile He_nV complex.[48] The He_4 cluster dissociates into several isolated atoms at 1500 K, which reveals that the high temperature may restrain the congregation of isolated helium and growth of clusters. In other word, the small helium clusters may be dissociated into several isolated atoms that are big enough to form He_nV complex. The He_nV complex becomes immobile which is conceived as the key for helium bubble nucleating and growth.[23] The formation of dislocation loop is accompanied by the growth of helium clusters.[35] The dislocation loop slides and annihilate on the surface to form adatom 'islands', conceived to be active during the initial stages of fuzz growth on tungsten.[23] Thus the high temperature may restrain the growth of helium clusters and eventually affects the formation of fuzz, which is in qualitative agreement with the conclusion of OKMC simulations.[41]

The behaviors of the He_6 cluster and tungsten self-interstitial atoms (SIAs) are shown in Fig. 3. One SIA forms a crowdion with ⟨111⟩ orientation around the He_6, and the

atomic configuration almost has no change except the random rotation of the He_6 cluster in the vacancy at 300 K, which looks as if the crowdion tightly attaches to the He_6 cluster. This reveals that a strong interaction exists between them as the crowdion and dislocation loop in tungsten have high mobility.[34] Boisse *et al.*[17] calculated the binding energy between them as ∼1.7 eV with DFT. At 1000 K, the crowdion rotates and changes its position relative to He_6, and even separates from the He_6 cluster as shown in Figs. 3(b) and 3(c). The crowdion quickly glides and occasionally rotates in the bulk, and the He_6 cluster has no obvious change at temperature 2000–3000 K within 628 ps, which are not shown here. At 3500 K, He_6 dissociates into separated helium atoms as shown in Fig. 3(d).

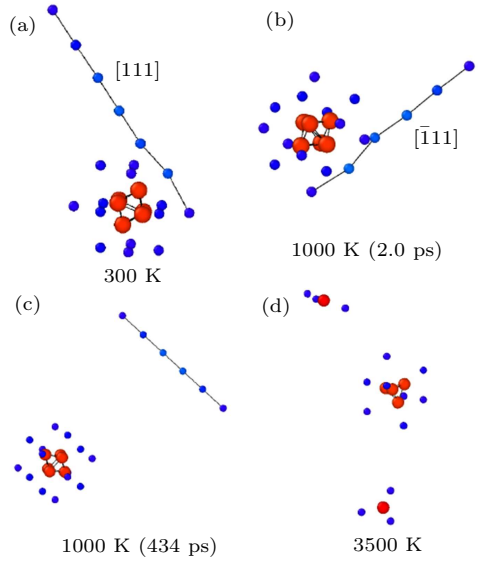

Fig. 3. The behaviors of SIAs and the He_6 cluster at different temperatures: (a) the crowdion and the He_6 cluster tightly bind at 300 K; (b) the crowdion rotates and rearranges its location around the He_6 at 1000 K; (c) the crowdion even diffuses away from the He_6 at 1000 K; (d) the crowdion is not shown here and the He_6 dissociates into several separated helium atoms at 3500 K. The bigger and smaller balls represent helium and tungsten, respectively. The colors of balls with rainbow represent atomic potential energies from −8.00 eV (blue) to 1.13 eV (red). The black sticks connect two atoms within the distances of 2.0 Å and 2.5 Å for He and W, respectively. Only the tungsten atoms with high potential energy are shown here for clarity.

The behaviors of the He_{13} cluster and tungsten SIAs are shown in Fig. 4. At 300 K, the SIAs tightly bind the He_{13}, and the atomic configuration almost has no change except the rotation of He_{13} cluster in the vacancy within 358 ps. The crowdion can rotate to change its relative position to the He_{13} at 1000 K. At 2000 K, the He_{13} cluster creates an extra SIA to form another crowdion to combine with the first crowdion. The two combined crowdions can rotate and change their position around the He_{13} as shown in Figs. 4(c) and 4(d). The behaviors of the helium cluster and SIAs at 3000 K are similar with those at 2000 K, which are not shown here. At 3500 K, an extra crowdion forms and the 3 crowdions separate from the He_{13} cluster and disperse themselves in the tungsten.

The behaviors of SIAs around He_{26} are shown in Fig. 5. Four SIAs are produced around the He_{26} cluster, and the configuration remains almost unchanged within 692 ps at temperature of 300 K. The configuration of four SIAs is still almost unchanged at 1000 K. It is found that the configuration of the He_{26} cluster has high symmetry as shown in Fig. 5(c). Different from the situations of He_6 and He_{13}, the $He_{26}V_4$ (V represent vacancy) complex is very stable and it does not rotate to change each helium's position. At 2000 K, the 4 SIAs self-assemble into 4 combined crowdions, which rotate and change their positions around the He_{26} cluster as shown in Figs. 5(d) and 5(e). The He_{26} cluster can create 5 and even 6 SIAs at temperature of 3000 K as shown in Figs. 5(f) and 5(g). The 5–7 SIAs can change their positions more quickly around the He_{26} cluster at 3500 K, which does not shown here.

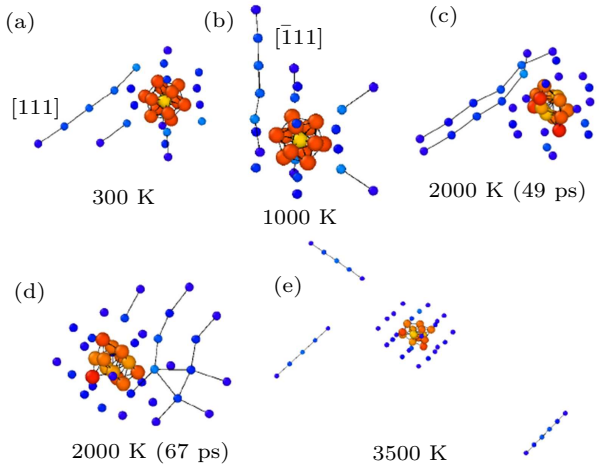

Fig. 4. The behaviors of SIAs and the He_{13} cluster at different temperatures: (a) one crowdion and He_{13} tightly combine at 300 K; (b) the crowdion rotates and rearranges its position around the He_{13} at 1000 K; (c) and (d) an extra Frenkel pair is created to form a two-combined crowdion which rotates and change its position at 2000 K; (e) an extra Frenkel pair is created, and three crowdions separate and diffuse away from the He_{13} at 3500 K. The graph settings are the same as Fig. 3.

The behaviors of SIAs around the He_{55} cluster at different temperatures are shown in Fig. 6. At 300 K, eight SIAs randomly disperse around the He_{55} cluster, and the atomic configuration is almost unchanged except helium within 723 ps. At 1000 K, the SIAs gradually gather at one side of the helium cluster and self-assemble into a dislocation loop (containing 10 SIAs along ⟨111⟩ crystal orientation). The dislocation loop can change its orientation between ⟨111⟩ and ⟨100⟩ orientations at 2000 K as shown in Figs. 6(c) and 6(d). The dislocation loop along the ⟨111⟩ orientation appears more frequently, indicating that the ⟨111⟩ configuration is more stable. At temperatures of 3000 K and 3500 K, the behaviors of the dislocation loop are similar to the situations of 2000 K, which are not shown here. The differences are that the He_{55} cluster can create more SIAs, 13–15 SIAs at 3000 K and 14–16 SIAs at 3500 K. It should be noted that the SIAs always stay at the same side of the helium cluster after forming dislocation loop even at 3500 K. In other words, the relative positions of dislocation loop and the He_{55} cluster are almost unchanged.

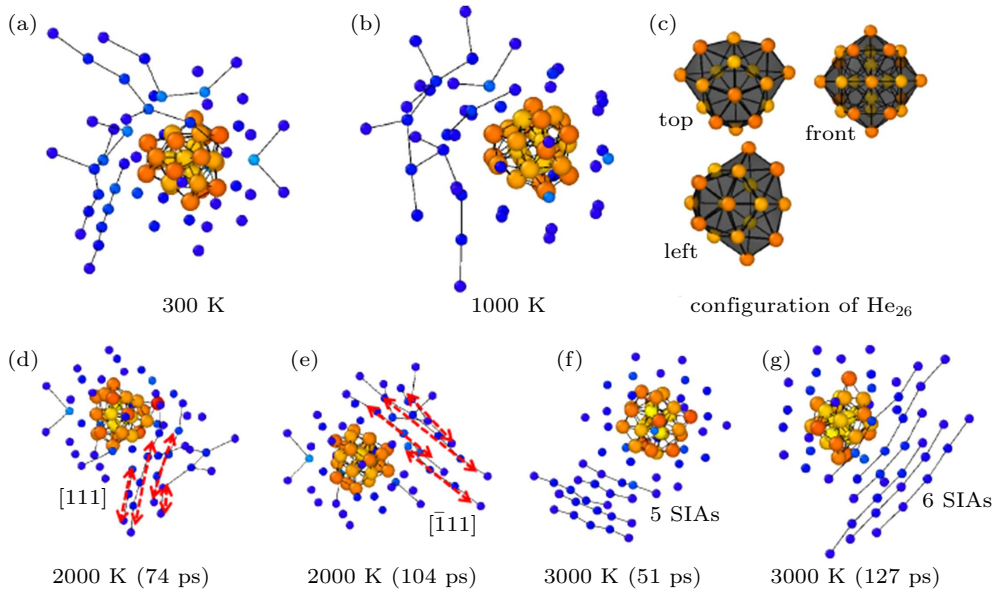

Fig. 5. The behaviors of SIAs around the He_{26} cluster at different temperatures. The configuration of dispersed crowdions is almost unchanged at (a) 300 K and (b) 1000 K; (c) the atomic structure of He_{26}; (d) at 2000 K, the SIAs change their positions and form a four-combined crowdion, and (e) the four-combined crowdion cluster rotates and changes its position; (f) extra one or (g) two Frenkel pairs are created to form a combined crowdion cluster at 3000 K, which can rotate and change its position around the He_{26}. The red arrows in the figure show the crowdions and their orientations. The graph settings are the same as Fig. 6.

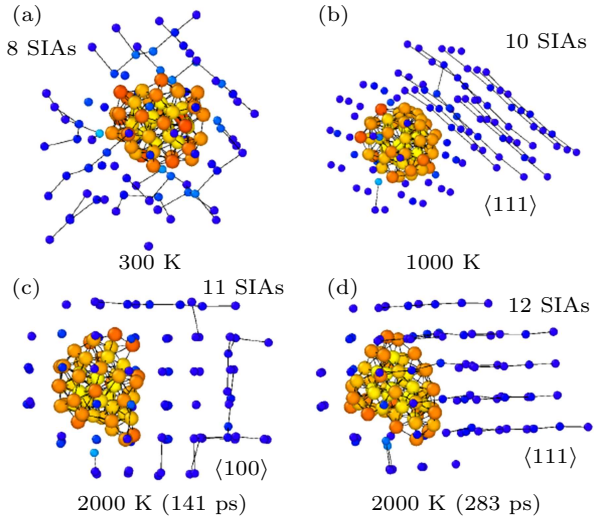

Fig. 6. The behaviors of SIAs around the He_{55} cluster at different temperatures: (a) eight insterstitial atoms disperse randomly around the He_{55} and the atomic structure is almost unchanged at 300 K; (b) the SIAs self-assemble and form a dislocation loop (containing 10 SIAs) at 1000 K; the dislocation loop can rotate between (c) ⟨100⟩ and (d) ⟨111⟩ orientations at 2000 K. The graph settings are the same as Fig. 3.

Table 1. The number of SIAs created by the He_n cluster at different temperatures. N_{SIA} and T represent the number of SIAs and temperature, respectively.

N_{SIA} \ T/K	300	1000	2000	3000	3500
He_6	1	1	1	1	–
He_{13}	1	1	2	2–3	2–3
He_{26}	4	4	4	5–6	5–7
He_{55}	8	10	12–13	13–15	14–16

The numbers of SIAs (Frenkel defects) created by the He_n cluster at different temperatures are listed in Table 1. It is found that the number of SIAs increases with the increasing temperature. For example, the He_{55} cluster creates 8 SIAs, 10 SIAs and 11–13 SIAs at 300 K, 1000 K and 2000 K, respectively. Boisse *et al.*[17] also suggested that the temperature and duration of simulation promote the trap mutation.

The displacements of mass center of helium clusters with evolution time at different temperatures are shown in Fig. 7. The displacements of He_6 show only slight fluctuation due to the atomic thermal vibration under 3000 K, and show large changes at 3500 K due to the dissociation of He_6. The center of mass of the He_{26} cluster shows large displacements at 3000 K and 3500 K due to the He_{26} creating extra 1–2 and 2–3 Frenkel defects at the corresponding temperatures. The displacements of the He_{13} and He_{55} clusters have the similar results. These results show that He_nV_m complex clusters can move by trap mutation at high temperature. Comparing the displacements of He_n cluster, we can find that the displacement of the He_n cluster decreases with the increasing size of helium clusters, which indicates that the stability of helium clusters increases with the size of helium clusters. The TEM *in situ* He ion irradiation experiment[27] also shows the low mobility of He-vacancy complexes at low temperature.

The SIAs created by helium clusters prefer to form crowdions, which self-assemble into dislocation loop (a bunch of crowdions) with preferential ⟨111⟩ crystal orientation at a medium temperature (1000–2000 K). The crowdions and dislocation loop always bind with helium clusters on the side which is the tensile region as suggested by Hammond *et al.*[36] such that the tensile region of dislocation loop attracts and traps helium. The crowdions and dislocation loop can rotate to change its position around the helium cluster at high temperatures, and even separate from helium clusters at more high temperature. In addition, a small helium cluster can dissociate

into several isolated helium atoms at high temperatures. All the main features of SIAs and helium clusters are listed in table 2. The bigger helium clusters create more SIAs. It is found that the temperatures for crowdions or dislocation loops to rotate increase with the size of dislocation loop. One crowdion rotates in the vicinity of He_6 and He_{13} clusters at 1000 K. Four combined crowdions rotate in the vicinity of He_{26} clusters at 2000 K. The twelve combined crowdions only change their orientations between ⟨100⟩ and ⟨111⟩ at 2000 K, which almost does not change their relative positions to He_{55} clusters. The results reveal that a big dislocation loop is more stable, which needs higher temperature to rotate. The results are consistent with our previous studies,[34] in which the rotating energy barriers increase with the increase of crowdions.

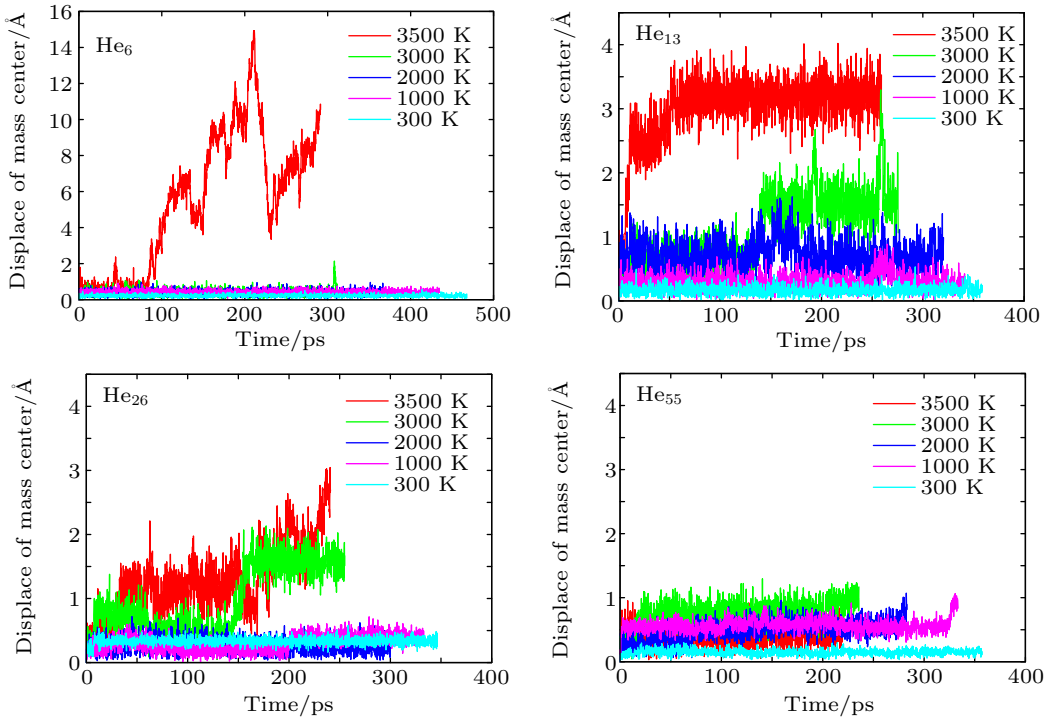

Fig. 7. The variations of displacement of mass center of the He_n cluster with evolution time at different temperatures.

Table 2. The main features of SIAs and helium clusters at different temperatures. The "rotation" represents the rotation of dislocation loop (or crowdions), the "separation" represents the crowdion separating from the helium cluster, and the "dissociation" represents the helium cluster dissociating into separated helium atoms. The figures in the parentheses represent the number of crowdions in rotation.

Events	Rotation	Separation	Dissociation
He_4 (0 crowdion)	–	–	1500 K
He_6 (1 crowdion)	1000 K	1000 K	3500 K
He_{13} (1 crowdion)	1000 K	3500 K	–
He_{26} (4 crowdions)	2000 K	–	–
He_{55} (12 crowdions)	2000 K	–	–

As shown in Table 2, it is found that the temperatures for dislocation loop (or crowdion) separating from the helium cluster increase with the size of helium clusters. The crowdion separates from the He_6 cluster at 1000 K, the 2–3 combined crowdions separate from the He_{13} cluster at 3500 K as shown in Fig. 4(e), and the 5–7 combined crowdions and dislocation loop (containing 14–16 crowdions) do not separate from He_{26} and He_{55} clusters even at temperature of 3500 K. The reasons may come from two aspects: (1) the strong binding energy between dislocation loop and helium cluster; (2) the bigger dislocation loop is more difficult to slide. According to our previous study,[34] the crowdion and dislocation loop (constructed with multiple crowdions) in pristine tungsten have extremely high mobility due to their very low slipping energy barriers (commonly less than 0.07 eV), and the slipping energy barriers are independent of the size of dislocation loop. Thus we speculate that the binding energies between dislocation loop and helium cluster increase with the size of helium clusters. We confirm our conjecture by calculating the binding energy of SIAs to helium clusters. The binding energy of SIAs with the helium cluster is defined as follows:

$$E_{\mathrm{b}} = E_{\mathrm{SIA}_m} + E_{\mathrm{He}_n\mathrm{V}_m} - (E_{\mathrm{He}_n\mathrm{V}_m+\mathrm{SIA}_m} + E_{\mathrm{ref}}), \tag{3}$$

where E_{SIA_m} represents the energy of m SIAs in pristine tungsten, $E_{\mathrm{He}_n\mathrm{V}_m}$ represents the energy of n He atoms in m vacancies, $E_{\mathrm{He}_n\mathrm{V}_m+\mathrm{SIA}_m}$ represents the energy of the combination of m SIAs and $\mathrm{He}_n\mathrm{V}_m$, and the E_{ref} represents the reference energy, which is the energy of pristine bulk tungsten. The binding energies of $\mathrm{He}_{13}\mathrm{V}_1$ to 1 SIA and $\mathrm{He}_{55}\mathrm{V}_{12}$ to 12 SIAs are calculated to be 1.13 eV and 13.35 eV, respectively. This shows that the big helium cluster has stronger binding energy with crowdions or dislocation loop. The strong binding between the helium cluster and the dislocation loop may be as

one possibility for the observable of dislocation loop in the TEM experiment.[27]

As shown in Table 2, the small helium clusters can dissociate into isolated helium atoms at high temperature, 1500 K for He_4 and 3500 K for He_6, while the big helium cluster is very stable, which does not dissociate even at temperature of 3500 K. The results indicate that the stability of helium clusters increases with the size. Compared with small helium clusters, big helium clusters are more stable, which is attributed to the lower atomic potential energy as shown in Fig. 1 and the stronger average binding energy as shown in Fig. 2.

4. Conclusions

We have conducted a molecular dynamics investigation on the size effect of He clusters on the interactions with self-interstitial tungsten atoms at different temperatures. The main conclusions are as follows:

High temperature promotes the occurrence of trap mutation of helium clusters.

Bigger dislocation loops are more stable, which need higher temperature to motivate rotation and change their position around the helium cluster.

The binding ability between the dislocation loop and the helium cluster increases with the size of helium clusters.

The stability of helium clusters increases with the increase of clusters. Our results can provide references for investigation on formation of fuzz with Monte Carlo simulation method.

References

[1] Sethian J D, Raffray A R, Latkowski J, Blanchard J P, Snead L, Renk T J and Sharafat S 2005 *J. Nucl. Mater.* **347** 161
[2] Bolt H, Barabash V, Krauss W, Linke J, Neu R, Suzuki S, Yoshida N and Team A U 2004 *J. Nucl. Mater.* **329–333** 66
[3] Nishijima D, Miyamoto M, Iwakiri H, Ye M Y, Ohno N, Tokunaga K, Yoshida N and Takamura S 2005 *Mater. Trans.* **46** 561
[4] Baldwin M and Doerner R 2008 *Nucl. Fusion* **48** 035001
[5] Nordlund K, Bjorkas C, Ahlgren T, Lasa A and Sand A E 2014 *J. Phys. D* **47** 224018
[6] Tokitani M, Yoshida N, Tokunaga K, Sakakita H, Kiyama S, Koguchi H, Hirano Y and Masuzaki S 2010 *Plasma Fusion Res.* **5** 012
[7] De Temmerman G, Bystrov K, Zielinski J J J, Balden M, Matern G, Arnas C and Marot L 2012 *J. Vac. Sci. Technol.* **30** 041306
[8] De Temmerman G, Bystrov K, Doerner R, Marot L, Wright G, Woller K, Whyte D and Zielinski J 2013 *J. Nucl. Mater.* **438** S78
[9] Baldwin M J and Doerner R P 2010 *J. Nucl. Mater.* **404** 165
[10] Yoshida N, Iwakiri H, Tokunaga K and Baba T 2005 *J. Nucl. Mater.* **337-339** 946
[11] Chen Z, Kecskes L J, Zhu K and Wei Q 2016 *J. Nucl. Mater.* **481** 190
[12] Abernethy R G 2017 *Mater. Sci. Technol.* **33** 388
[13] Becquart C and Domain C 2006 *Phys. Rev. Lett.* **97** 196402
[14] Becquart C and Domain C 2009 *J. Nucl. Mater.* **385** 223
[15] Tamura T, Kobayashi R, Ogata S and Ito A M 2014 *Modell. Simul. Mater. Sci. Eng.* **22** 015002
[16] Liu Y, Zhou H, Zhang Y, Jin S and Lu G 2009 *Nucl. Instrum. & Methods Phys. Res. Sect. B-beam Interact. Mater. Atoms* **267** 3193
[17] Boisse J, Domain C and Becquart C 2014 *J. Nucl. Mater.* **455** 10
[18] Smirnov R, Krasheninnikov S and Guterl J 2015 *J. Nucl. Mater.* **463** 359
[19] Zhou Y, Wang J, Hou Q and Deng A 2014 *J. Nucl. Mater.* **446** 49
[20] Hu L, Hammond K D, Wirth B D and Maroudas D 2014 *J. Appl. Phys.* **115** 173512
[21] Hu L, Hammond K D, Wirth B D and Maroudas D 2014 *Surf. Sci.* **626** L21
[22] Perez D, Vogel T and Uberuaga B P 2014 *Phys. Rev. B* **90** 014102
[23] Sefta F, Hammond K D, Juslin N and Wirth B D 2013 *Nucl. Fusion* **53** 073015
[24] Wang J, Niu L L, Shu X and Zhang Y 2015 *Nucl. Fusion* **55** 092003
[25] Kobayashi R, Hattori T, Tamura T and Ogata S 2015 *J. Nuclear Materials* **463** 1071
[26] You Y, Li D, Kong X, Wu X, Liu C S, Fang Q F, Pan B C, Chen J and Luo G N 2014 *Nucl. Fusion* **54** 103007
[27] Harrison R W, Greaves G, Hinks J and Donnelly S 2017 *J. Nucl. Mater.* **495** 492
[28] Takayama A, Ito A M, Saito S, Ohno N and Nakamura H 2013 *Jpn. J. Appl. Phys.* **52** 01AL03
[29] Zhan J, Ye M, Mao S, Ren J and Xu X 2019 *Fusion Engineering and Design* **146** 983
[30] Pentecoste L, Brault P, Thomann A L, Desgardin P, Lecas T, Belhabib T, Barthe M F and Sauvage T 2016 *J. Nucl. Mater.* **470** 44
[31] Mason D R, Yi X, Kirk M A and Dudarev S L 2014 *J. Phys.: Condens. Matter* **26** 375701
[32] Kong X, Wu X, You Y, Liu C S, Fang Q F, Chen J, Luo G N and Wang Z 2014 *Acta Mater.* **66** 172
[33] Derlet P M, Nguyen-Manh D and Dudarev S 2007 *Phys. Rev. B* **76** 054107
[34] Wang J, He B, Song W and Dang W 2019 *Mol. Simul.* **45** 666
[35] Wang J, Niu L L, Shu X and Zhang Y 2015 *J. Phys.: Condens. Matter* **27** 395001
[36] Hammond K D, Ferroni F and Wirth B D 2017 *Fusion Sci. Technol.* **71** 7
[37] Li X, Liu Y, Yu Y, Luo G, Shu X and Lu G 2014 *J. Nucl. Mater.* **451** 356
[38] Sandoval L, Perez D, Uberuaga B P and Voter A F 2015 *Phys. Rev. Lett.* **114** 105502
[39] Kajita S, Sakaguchi W, Ohno N, Yoshida N and Saeki T 2009 *Nucl. Fusion* **49** 095005
[40] Nishijima D, Ye M Y, Ohno N and Takamura S 2004 *J. Nucl. Mater.* **329-333** 1029
[41] Valles G, Martin-Bragado I, Nordlund K, Lasa A, Björkas C, Safi E, Perlado J and Rivera A 2017 *J. Nucl. Mater.* **490** 108
[42] Plimpton S 1995 *J. Comput. Phys.* **117** 1
[43] Stukowski A 2009 *Modell. Simul. Mater. Sci. Eng.* **18** 015012
[44] Bonny G, Grigorev P and Terentyev D 2014 *J. Phys.: Condens. Matter* **26** 485001
[45] Juslin N and Wirth B D 2013 *J. Nucl. Mater.* **432** 61
[46] Voter A F 1998 *Phys. Rev. B* **57** R13985
[47] Voter A F, Montalenti F and Germann T C 2002 *Annu. Rev. Mater. Res.* **32** 321
[48] Krasheninnikov S, Faney T and Wirth B 2014 *Nucl. Fusion* **54** 073019